Title
Modeling and Test Validation of a 15kV 24MVA Superconducting Fault Current Limiter

Authors
Moriconi, Franco
Singh, Amandeep
Rosa, Francisco De La
et al.

Publication Date
2010

Modeling and Test Validation of a 15kV 24MVA Superconducting Fault Current Limiter

Franco Moriconi, Nick Koshnick, Francisco De La Rosa, *Senior Member, IEEE* and Amandeep Singh, *Member, IEEE*

Abstract--**High-power short-circuit test results and numerical simulations of a 15kV-24MVA distribution-class High Temperature Superconductor (HTS) Fault Current Limiters (FCL) are presented and compared in this paper. The FCL design was based on the nonlinear inductance model here described, and the device was tested at 13.1kV line-to-line voltage for prospective fault currents up to 23kArms, prior to its installation in the electric grid. Comparison between numerical simulations and fault test measurements show good agreement. Some simulations and field testing results are depicted. The FCL was energized in the Southern California Edison grid on March 9, 2009.**

Index Terms-- **Air-core inductance, electromagnetic model, fault current limiter, finite elements, nonlinear impedance, saturable core, short circuit, superconductivity, voltage drop.**

I. Nomenclature

HTS – High Temperature Superconductor
FCL – Fault Current Limiter
FEM – Finite Element Methods

II. Introduction

ELECTRIC utilities are constantly searching for ways to maintain a balance between increased fault current levels and circuit breaker interrupting capabilities. The addition of transformation capacity at a substation bus, for example, increases the available short-circuit current. Rated circuit breaker interrupting capabilities can be exceeded earlier than planned with adverse implications such as excessive mechanical forces and heating on switchgear during faults.

Replacement of existing breakers and other equipment by larger units with increased fault current level is always an option. However, this may become a costly solution, especially in transmission or sub-transmission applications.

Among other alternatives utilities have more recently considered is the use of fault current limiters to reduce the peak of the fault current. This has become an area of active research and development, and there are pilot applications to assess the proof of concept of different designs. These devices, which are typically on the path between substation busses or off distribution feeders at the substation, are non-linear systems and they change state between low and high impedance at the time of a short circuit condition. Fault current limiters can offer tangible benefits to power utilities, especially in cases where circuit breakers are approaching, or even worse – exceeding rated interrupting levels.

The HTS FCL here presented is a saturable core reactor [1] efficiently designed and customized to present low voltage drop under normal operating conditions, and to generate significant fault current reduction under line-to-ground or line-to-line fault currents. The FCL is designed to operate as an inherently variable reactance based on the fact that its insertion impedance is proportional to the relative permeability of the magnetic iron core used. Under normal operating conditions the FCL has a very low series reactance, but under fault conditions the reactance instantly changes to a very high value in order to limit the current surge to a desired safe level. When the fault is cleared, the operating point automatically returns to its normal state corresponding to a very low series reactance, hence a low voltage drop during steady state.

Fig. 1 shows a single-phase arrangement of the FCL. An HTS coil provides the DC bias to saturate the two cores of every phase. For the 15kV FCL device a three-phase configuration shown in Fig. 2 was realized with six core limbs, two per phase, passing through a single DC coil.

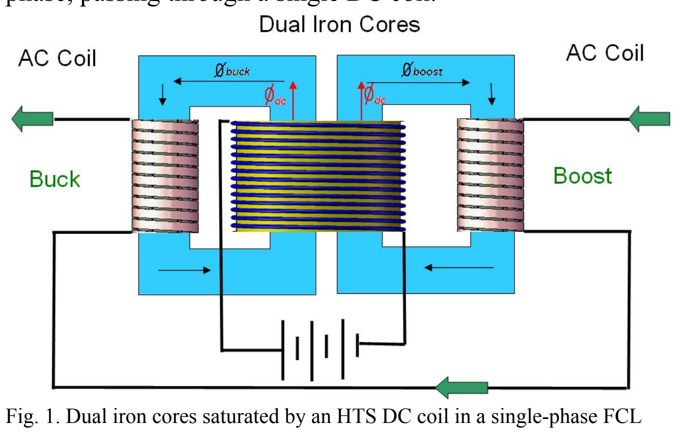

Fig. 1. Dual iron cores saturated by an HTS DC coil in a single-phase FCL

This work was supported in part by the California Energy Commission.

F. Moriconi, N. Koshnick, F. De La Rosa, and A. Singh are with Zenergy Power, Inc., South San Francisco, CA, USA.

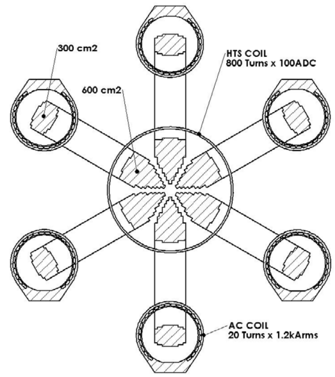

Fig. 2. 15kV three-phase FCL saturated by an HTS DC coil

III. FCL NONLINEAR INDUCTANCE MODEL

Saturable core FCLs consist of a set of coils wound around one or more paramagnetic cores. A superconducting magnet is coupled to the core region in such a way that the DC magnetization force can saturate the magnetic material. In Zenergy Power's FCL, each AC phase consists of two coils connected in series and wound around two core regions. The windings are oriented such that, in one core, positive AC current counteracts (bucks) the superconducting DC bias while, in the other core, negative AC current assists (boosts) the superconducting DC bias.

The nonlinear model which describes the behavior of the device is based on the physical principle described above. The core material has B-H characteristics that can be approximated by an inverse tangent function. We begin by estimating the linkage magnetic field in the core section seen by one AC coil as:

$$B(i_{ac}) = \frac{-2B_{sat}}{1+\tan^{-1}\left(K\pi - \frac{\pi}{2}\right)}\left[1+\tan^{-1}\left(K\frac{\pi}{I_{\max}}(I_{\max}-i_{ac})-\frac{\pi}{2}\right)\right]+2B_{sat}$$

where i_{ac} is the instantaneous AC line current, I_{max} is the line current it takes to fully saturate the cores, at which point the average magnetic field is B_{sat}, and K determines the range of line currents where the magnetic state of the cores are actively changing from saturate to unsaturated. The equation is scaled in such a way that B = 0 at i_{ac} = 0 (bias point), and the majority of the change in field occurs just before $i_{ac} = I_{max}$.

The induced voltage, or back emf, across this section of the FCL is $V = \widetilde{L}\partial i/\partial t$ where $\widetilde{L}$ is the differential inductance defined as:

$$\widetilde{L} = n_{ac} A_{core} \frac{\partial B(i_{ac})}{\partial i_{ac}}$$

Here, n_{ac} is the number of turns in the ac coil, which carries the line current, and A_{core} is the cross-sectional area of the paramagnetic core material. In some cases, this model is improved by imposing two additional conditions. First, $\widetilde{L}$ must be greater than or equal to an additional parameter called L_{air}. This value represents the insertion impedance as an equivalent air-core inductance. Furthermore, if i_{ac} is greater than I_{max}, then $\widetilde{L}$ is constrained to be L_{air}. This accounts for the fact that, when the line current is very large, the FCL's magnetic core is reverse saturated and the impedance is once again approximately equal to the insertion impedance of an equivalent air-core inductor.

The equations above provide a general framework for describing the behavior of an FCL in an electric circuit. This framework requires four input parameters: I_{max}, B_{sat}, K, and L_{air}. As described in the following sections, we use finite element methods (FEM) simulations to calculate the average magnetic flux for various static values of superconducting-currents and line currents. We then take these flux values and use a least squares fitting procedure to determine the above parameters. Finally, we use some form of electrical simulation software (such as PSCAD®) to implement the nonlinear inductance model and compare it to experimental results from the extensive tests perform on the 15kV FCL device.

IV. FEM MODEL AND ANALYSIS

A. FEM Model

Precise FEM results require a number of inputs, including physical geometry, accurate descriptions of the electromagnetic properties of each material, and the current densities in the superconducting and AC coils. Calculations were performed using the ANSYS® FEM code. The geometric parameters were either input directly from mechanical CAD drawings or by command files. Because the designs have many elements, calculation speed is a significant constraint. In most cases our models make use of geometric symmetries to improve the calculation speed. The B-H curve for the magnetic material was estimated from measured data shown in Fig. 3. All calculations discussed in this paper were performed under the static approximation. This assertion is justified by the fact that physical devices do no display significant hysteretic behavior.

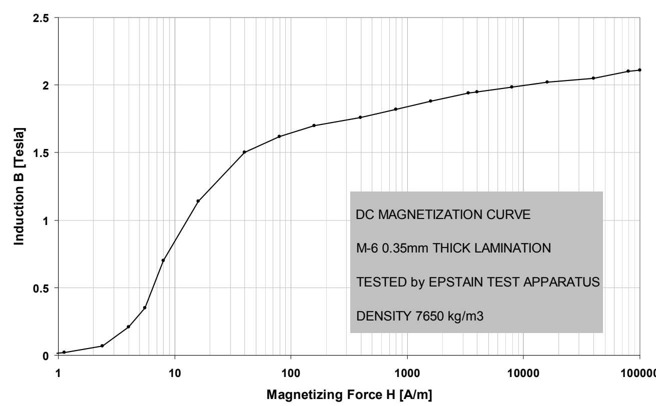

Fig. 3. DC Magnetization Curve of M-6 Steel used in FEM model

The ANSYS®'s LMATRIX subroutine [3] provides the differential inductance matrix for the number of coils present in the model, and the total flux linkage in each coil, under a given set of current density conditions. The FEM model provides graphical outputs like the one shown in Fig. 4 that allow easy visualization of geometric properties. Graphical outputs also provide insight for future designs by allowing us to analyze magnetic field densities in each region (Fig. 5). After using the graphical outputs to verify the model is working well, we use either the flux or the inductance outputs to calculate the parameters for the nonlinear voltage model.

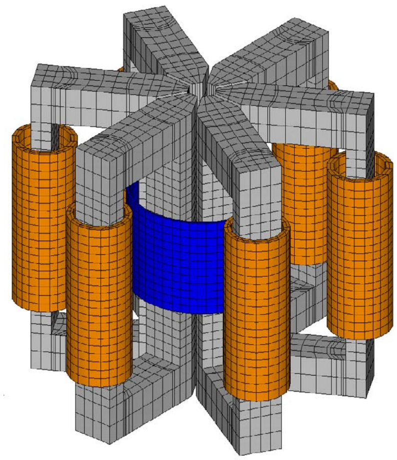

Fig. 4. Finite element model of a 15kV three-phase FCL. The (grey) iron cores serve as flux links between the (blue) superconducting magnet in the center of the device and the (orange) AC coils. This three phase device has six AC coils in total; one boosting coil and one bucking, coil for each phase at any given time.

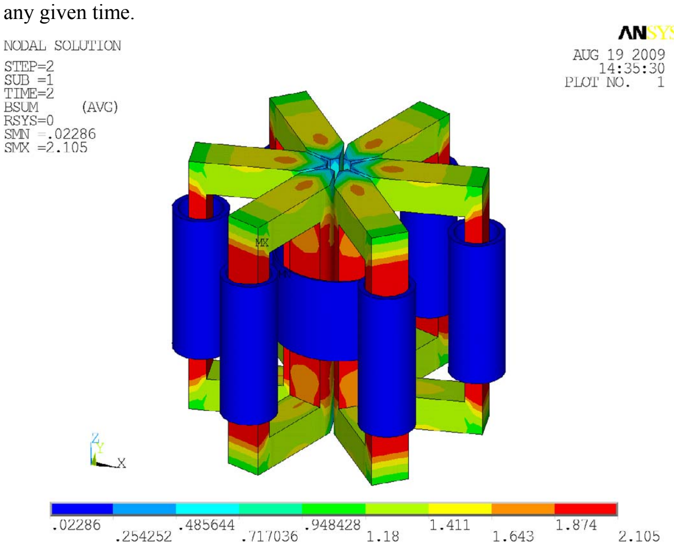

Fig. 5. Total flux density due to DC Magnetization at 80,000 Amp-turns.

B. Analysis

FEM analysis allows us to model our devices before they are constructed. We calculate a series of flux or inductance values over a range of AC and DC currents. The data points shown in Fig. 6 were calculated for a superconducting bias current of 100 amps, or 80,000 amp-turns. The process can be repeated for other superconducting DC bias points if necessary. Figure 6a shows the average magnetic field linking the boosting and bucking coils. The values were calculated from flux values, $\Phi(i_{ac})$, with the equation $B_{ansys} = \Phi(i_{ac})/n_{ac}A_{core}$. In this case, $n_{ac} = 20$ turns and $A_{core} = 300$ cm^2. Figure 6b shows the sum of these magnetic fields. The inductance values shown in figure 6c were calculated from 6b with the relation:

$$L = n_{ac}\, A_{core}\, B(i_{ac})/i_{ac}$$

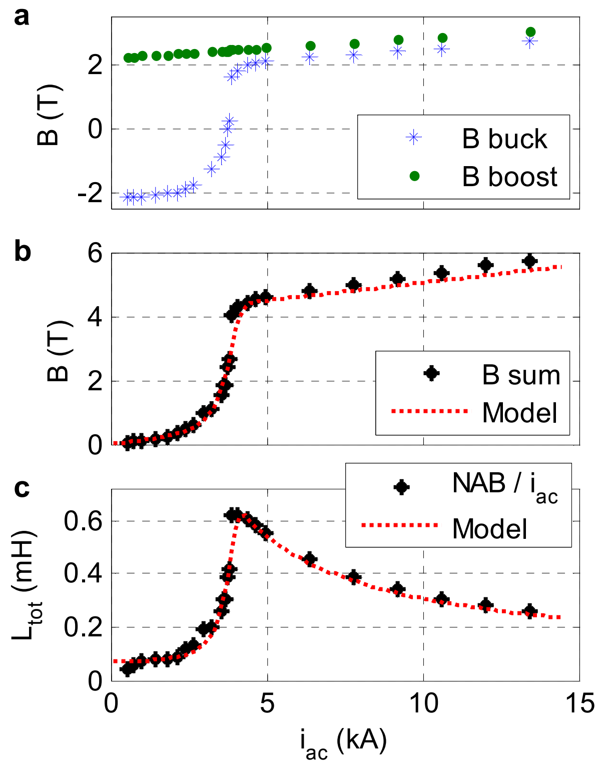

Fig. 6. FEM simulated results and model fitting. a) Average flux density through the AC coils for various AC current values when 80,000 amp-turns are applied to the superconducting magnet. b) The sum of the two average B-fields shown in figure a. The dotted line is a best fit to the non-linear model in section 2 with B_{sat} = 2.09 Tesla, L_{air} = 33.6 μH, I_{max} = 4.38 kA, and K = 3.73. c) The FEM generated inductance. The dotted line represents the same model with best fit parameters B_{sat} = 2.11 Tesla, L_{air} = 36.2 μH, I_{max} = 4.28 kA, and K = 4.48.

The dotted red lines in figure 6b show the model described in section II applied to both the boosting and bucking cores. A similar fit was obtained for the inductance values shown in figure 6c. This inductance is related to the differential inductance by $L = \frac{1}{i_{ac}}\int_0^{i_{ac}} \tilde{L}(i)di$, which was performed numerically to account for the conditional statements applied to our differentially defined inductance when $i_{ac} > I_{max}$ and $\tilde{L} < L_{air}$. In the following section we will use the best-fit values from the inductance fit to compare this model to the measured behavior of the FCL device.

V. EXPERIMENTAL RESULTS AND MODEL VALIDATION

Short circuit tests of Zenergy's 15kV FCL took place at Powertech Laboratories in British Columbia, Canada. The three-phase FCL was connected to the test source voltage as shown in Fig. 7, and an auxiliary breaker provided the fault current by closing the three-phase-to-ground fault at the appropriate point-on-wave. Source resistance and reactance were selected to provide the necessary prospective fault current levels with the required asymmetry factor.

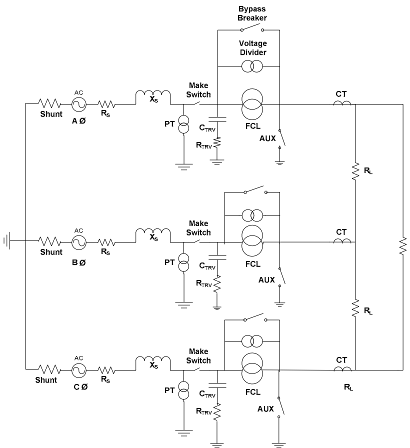

Fig. 7. High-power short-circuit FCL test set up.

Fig. 8 shows two cycles of load current followed by the first two cycles under faulting conditions. Figures 8a and 8b show a 6.5 kV line-to-line system with a 3 kA rms and a 12.5 kA rms prospective fault, respectively. Fig. 8c shows a 13.1 kV line-to-ground system with a 20 kA rms prospective fault. All tests were performed with an Xs/Rs ratio greater than 20. After briefly describing the test circuit we will describe the symmetrical fault limiting performance of the model in figures 9 and 10.

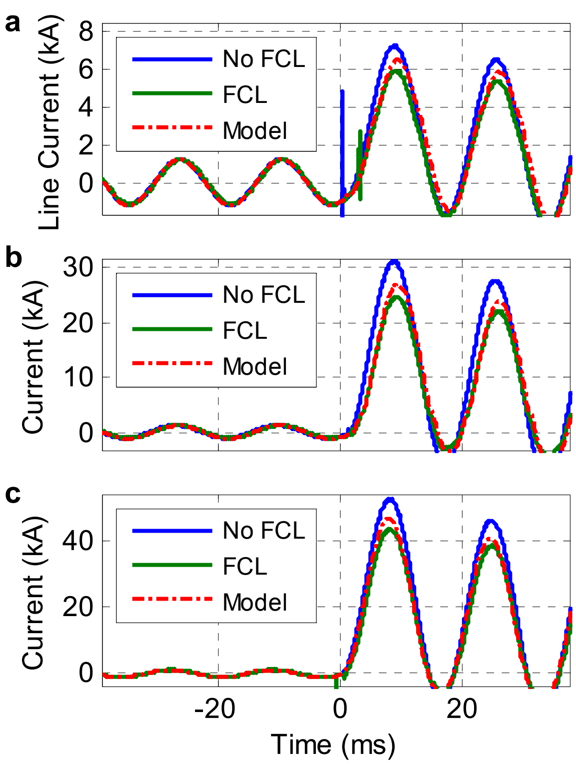

Fig. 8. Measured and modeled current as a function of time. a) A 6.5 kV line to line system with two 830 Arms load cycles followed by a 3 kArms prospective fault. The symmetrical part of the fault current was limited by 17%. b) The same system with two 825 Arms load periods followed by a 12.5 kArms prospective fault. The FCL limited 30% of the symmetrical prospective fault current. c) A 13.1 kV line-to-line system, with two 780 Arms load cycles followed by a 23 kArms prospective fault where the FCL limited 20% of the symmetrical current. The dotted red lines use the parameters derived from FEM modeling.

We have analyzed the experimental results using a simplified lump-sum circuit that consists of a voltage source, the nonlinear voltage FCL model, and a time-dependent load resistor. The idealized source has the voltages listed above and a source impedance of 0.8 mH and 14 mΩ. The FCL includes the current-dependent inductance described above along with a resistance of 1 mΩ. The simplified model's load impedance was chosen to generate the correct current during the loading cycles. This impedance was switched to zero during the fault cycles.

We have found that the nonlinear FCL voltage model can quantitatively reproduce the measured results. The FEM analysis provides a concrete method for estimating the model parameters for the saturated core FCL design. The estimated parameters were used for the modeled results shown in figures 8 and 9. Fig. 9 shows the symmetrical fault current after 21 cycles of continuous energization. At this point, the estimated parameters provide excellent predictions for overall fault current reduction. The qualitative features of the FCL voltage response are also estimated well as shown in 9b. Fig. 9c shows the average magnetic field defined by the measured flux change (i.e. the integrated bushing-to-bushing measured voltage with respect to time) divided by $n_{ac}A_{core}$. While the qualitative features of the magnetic field are reproduced by the model, the quantitative agreement is not precise.

We have increased the accuracy of our model by adjusting the input parameters to match the measured response. Figure 10 demonstrates the qualitative agreement that is possible after the model updating.

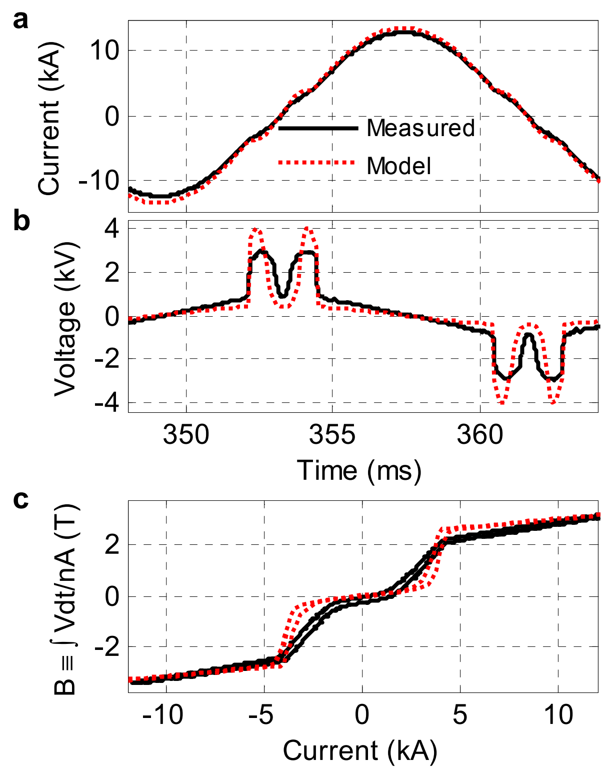

Fig. 9. Measured and modeled current (a) and voltage (b) as a function of time for a 12.5 kA rms symmetrical prospective fault after 21 cycles or 350 ms. c) Average magnetic field as computed from the integral of the measured FCL back emf with respect to time. The modeled values used the following FEM modeling-derived parameters: B_{sat} = 2.11 T, L_{air} = 36.2 μH, I_{max} = 4.28 kA, and K = 4.5.

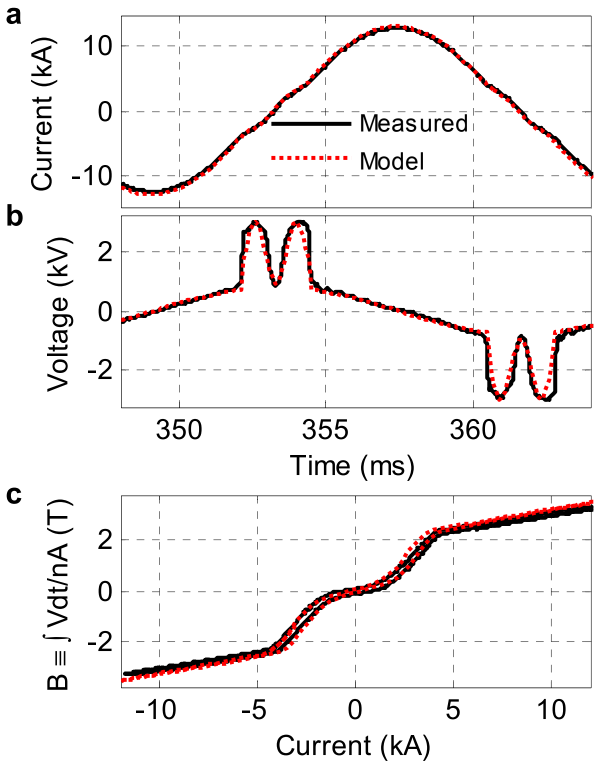

Fig. 10. Measured and modeled current, voltage, and integrated B-field under the same conditions shown in figure 9. We found excellent agreement between the model and measured values with the following input parameters. B_{sat} = 1.8 T, L_{air} = 70 μH, I_{max} = 4.3 kA, and K = 1.5.

The device described above was delivered to Southern California Edison (SCE) in January 2009. On March 9, 2009, SCE energized the FCL in the Avanti Circuit of the Future, bringing on-line the first superconducting FCL in the US electrical grid. In a subsequent paper we plan to report on the operating experience at the Circuit of the Future.

VI. Subsequent Development

The modeling prescription described above has allowed Zenergy Power to improve the design and the performance of a second-generation saturated-core HTS FCL. We are currently working on an innovative FCL design that offers improved fault current limiting performance while at the same time occupying a smaller physical form factor. Full-scale 15kV prototype units of this new design performed extremely well in early fault current testing. They showed exceptionally low insertion impedance at maximum load currents and significantly improved fault current limiting capability. A three-phase compact FCL configuration showed less than 70V voltage drop at 1.2kA rms load current and a fault limiting capability of 46% at 25kA symmetrical prospective fault current, as shown in Fig. 11. The back emf during faults showed peak values of the order of 4kV with no signs of reverse core saturation. This indicates that our modeling allowed us to properly size the magnetic cores and the number of AC turns for the available DC ampere-turns.

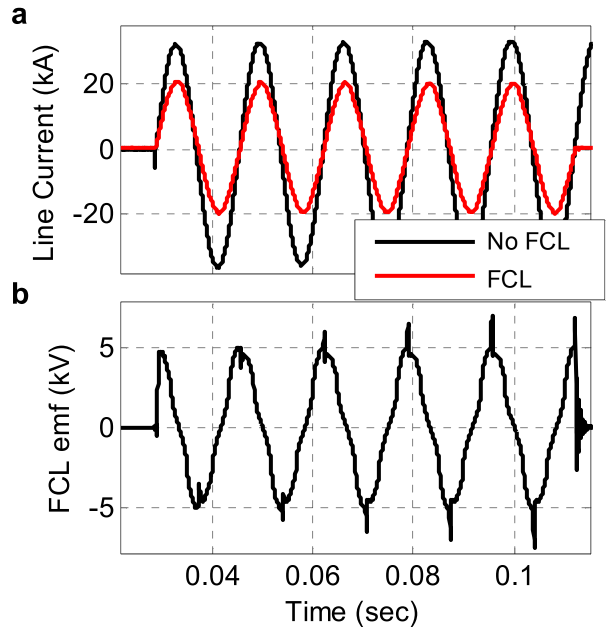

Fig. 11. Fault currents and FCL back emf as a function of time. The black line shows a 25 kA rms prospective fault which was limited to 13.5 kA rms by the FCL (red), a 46% fault current reduction. Test line voltage was 13.1kV line-to-line.

VII. Conclusions

We have presented a systematic approach to model the electrical behavior of a saturated core HTS fault current limiter. The physically motivated model was supported with FEM electromagnetic simulations and circuit analysis in order to predict and then match experimental results. The nonlinear FCL voltage model, with the FEM updated parameters, provides an excellent tool for predicting the overall fault current reduction of a saturated core HTS fault current limiter.

The FCL model was used by Zenergy Power in designing an innovative distribution class 15kV saturated core FCL that in full-scale testing showed fault current limiting capabilities close to 50% of 25kA prospective fault currents, while maintaining the voltage drop, or insertion impedance, below 1% of the line voltage for load currents of 1.2kA rms.

The FCL described above was energized and inserted in the Southern California Edison Circuit of the Future on March 9, 2009. This superconducting FCL is the first to be energized in the US electrical grid.

VIII. References

[1] A Current Limiting Device Using Superconducting D.C. Bias Applications and Prospects, Raju, B.P. Parton, K.C. Bartram, T.C.., IEEE Transactions on Power Apparatus and Systems, Sept. 1982.

[2] Model of HTS three-phase saturated core fault current limiter, Keilin, V. Kovalev, I. Kruglov, S. Stepanov, V. Shugaev, I. Shcherbakov, V. Akimov, I. Rakov, D. Shikov, A. Kurchatov (I.V.) Inst. of Atomic Energy, Moscow - IEEE Transactions on Applied Superconductivity Publication Date: Mar 2000

[3] Inductance Computation by Incremental Finite Element Analysis", IEEE Transactions on Magnetics, Vol.35. No.3. pp.1119-22, May 1999.

[4] Simulation of HTS Saturable Core-Type FCLs for MV Distribution Systems, S. B. Abbott, Member, IEEE, D. A. Robinson, S. Perera, Member, IEEE, F. A. Darmann, C. J. Hawley, and T. P. Beales. IEEE Transactions on Power Delivery, VOL. 21, NO. 2, APRIL 2006.

IX. BIOGRAPHIES

Franco Moriconi leads Zenergy's Engineering effort in the development of a commercial Superconducting Fault Current Limiter. Under his technical leadership Zenergy Power installed and energized a first-ever HTS FCL in the US electric grid. In 1992, he joined ABB Corporate Research to lead R&D work in the areas of numerical and Finite Elements methods, short-circuit strength and noise reduction of power transformers, Gas Insulated Switchgear technology, and high-speed electrical motors and generators. He also participated in two IEC working groups, and was the Convener of the IEC Scientific Committee 17C on seismic qualification of GIS. Currently, he is an active member of the IEEE Task Force on FCL Testing. Franco Moriconi earned a Bachelor of Science degree and a Master of Science degree in Mechanical Engineering from UC Berkeley. He is the co-author of six patents in the field of HV and MV electrical machines.

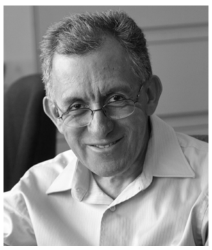

Francisco De La Rosa joined Zenergy Power, Inc. in April 2008 at the time the Company was embarked in the development of the first HTS FCL prototype that would become a utility tested unit. He has held various positions in R&D, consultancy and training in the electric power industry for around 30 years. His fields of interest include the smart grid concept, applications of superconductivity in power systems, power quality, and power system protection in utilities and industry. He is a Collective Member of CIGRE and a Senior Member of IEEE PES where he contributes in several Working Groups.

Amandeep Singh has been with Zenergy Power Inc. since January 2008. He holds a Bachelor of Electronics & Telecommunications degree from GNEC, Ludhiana (Punjab). He has worked for ten years in utility generation, transmission and distribution sectors for plant control systems, sub-station O&M and distribution system planning, augmentation, metering and revenue handling. He has an EIT in the State of California and is pursuing a professional engineer's registration. He is a member of IEEE.

Nick Koshnick is a consulting engineer with Zenergy Power with expertise in electrical and electromagnetic modeling and superconductivity. He earned a PhD in applied Physics from Stanford University in early 2009.